BSD-TDR-63-124

REPORT NO.
TDR-169(3153-20)TN-1

Flight Instrumentation for Reentry Plasma Sheath

12 JULY 1963

Prepared by ALLEN E. FUHS
Plasma Research Laboratory

Prepared for COMMANDER BALLISTICS SYSTEMS DIVISION
UNITED STATES AIR FORCE
Norton Air Force Base, California

LABORATORIES DIVISION • AEROSPACE CORPORATION
CONTRACT NO. AF 04(695)-169

BSD-TDR-63-124

Report No.
TDR-169(3153-20)TN-1

FLIGHT INSTRUMENTATION FOR REENTRY PLASMA SHEATH

Prepared by

Allen E. Fuhs
Plasma Research Laboratory

AEROSPACE CORPORATION
El Segundo, California

Contract No. AF 04(695)-169

12 July 1963

Prepared for

COMMANDER BALLISTICS SYSTEMS DIVISION
UNITED STATES AIR FORCE
Norton Air Force Base, California

ABSTRACT

A number of instruments for probing the plasma sheath during reentry are described. The instruments respond to the induced magnetic field produced by the interaction of the ionized gas flowing through an applied magnetic field. Flight models to measure the product of electrical conductivity and velocity, σu, and the σu profile are discussed. In addition analysis and description of laboratory transducers for determining velocity, σu fluctuations, and average electron collision frequency are presented.

CONTENTS

NOMENCLATURE . . . . . .

I. INTRODUCTION 1

II. DISCUSSION OF PLASMA SHEATH 3

A. Parameters Influencing the Plasma Sheath 3

B. Parameters Characterizing the Plasma Sheath 5

III. FLIGHT INSTRUMENTATION DEVELOPED AT PLASMA RESEARCH LABORATORY 9

A. Relation of Signal to Flow Properties 9

B. Average σu Transducers 11

C. Conductivity/Velocity Profile Meter 19

D. Flow Angle Indicator 22

E. Average Electron Collision Frequency 26

F. Velocity Measurement 27

G. Turbulence Indicator 31

IV. SUMMARY 33

ACKNOWLEDGEMENT 35

REFERENCES 37

TABLES

1. Electron Densities for Different Trajectories 4

2. Data for Plasma Sheath on Sharp Cone 6

FIGURES

1	Transducer Coil Arrangement	10
2	Flow Field and Location of Transducer on Reentry Vehicle	13
3	Observed Value of $\overline{\sigma u}$ and the Angle of Attack of the Reentry Vehicle	14
4	Average σu Transducer Geometry Readily Adaptable to Cone Designs	15
5	Cancellation of Earth's Magnetic Field and Addition of Induced Magnetic Field due to Plasma Flow	17
6	Flight Instrument to Measure $\overline{\sigma u}$. Transducer, 8 lb; Electronics Box, 2.5 lb; Compensation Box, 1 lb	18
7	Illustration of the Results of a Calculation of σu Profile	20
8	A Coil Geometry Providing Three Different Scale Primary Fields	21
9	Comparison of Actual and Measured Profiles	23
10	MHD Electrical Conductivity/Velocity Profile Meter	24
11	Crossed Sensing Coil Geometry	25
12	The Excitation of the Primary Field and the Anticipated Signal	28
13	Velocity and Turbulence Transducer	29
14	Typical Signals from Velocity Transducer	30

NOMENCLATURE

A	cross sectional area of sensing coil, m^2
B, $\vec{B}$	magnetic flux density, Wb/m^2
$\vec{E}$	electric field, V/m
e	sensing coil electromotive force, V
F	cross correlation function
$\vec{J}$	current density, amp/m^2
K, K(y)	influence function, V/(mho/m)(m/sec)(m)
L	characteristic transducer length, m
N	number of turns
n	sensing coil normal
N_e	electron density, m^{-3} or cm^{-3}
R	primary coil radius, m
r	distance between current element and point where magnetic flux density is to be determined, m
t	time, sec
u, $\vec{u}$	flow velocity, m/sec
V	volume, m^3
x, y, z	spatial coordinates, m
α	angular position of coil relative to reference axis
δ	boundary layer thickness; shock layer thickness, m
ϵ	electrical permittivity, F/m
θ	angle of flow relative to reference axis
μ	magnetic permeability, H/m

NOMENCLATURE (Continued)

ν	electron-neutral collision frequency, sec^{-1}
σ	electrical conductivity (scalar or tensor), mho/m
σ'	electrical conductivity (scalar), mho/m
τ	time (see Eq. 11), sec
ω	frequency, rad/sec

Subscripts

i, j	indices
o	free space value
c	cyclotron
p	plasma

I. INTRODUCTION

Surrounding high speed vehicles within the earth's atmosphere is a plasma sheath arising from the heating of air in the shock-wave, in the boundary layer, or in separate shear layers. The plasma sheath, which completely encases the vehicle and feeds the wake that extends downstream many body diameters, interferes with radio communication to and from the vehicle. These facts have been well known to the professional missileman and space scientist for many years; since the Mercury flights, the facts are equally familiar to the layman.

In addition to communication blackout, the plasma sheath causes other problems. Less dense plasmas, while not causing blackout, have adverse effects on electromagnetic wave propagation, including refraction of the waves, introduction of noise, distortion of antenna patterns, and mismatch of antennas. The radar cross section of a reentry vehicle may be enhanced by one, two, or three orders of magnitude depending on the radar frequency and the reentry vehicle. Refraction of the electromagnetic waves may make angular information from on-board radar of questionable value.

However, the plasma sheath is not entirely detrimental. Magnetoaerodynamic attitude control attempts to exploit this flow of conducting gases by developing forces on the vehicle. The advent of practical superconducting coils has caused renewed interest in this aspect of attitude control. The plasma sheath also makes possible magnetohydrodynamic (MHD) power generation. If one considers the enormous amount of kinetic and potential energy dissipated during reentry, it is apparent that only a small fraction of this energy need be extracted to have megawatts of power.

This paper reports on flight instrumentation being developed to gain information about the reentry plasma sheath. Discussion of the plasma sheath is continued in Section II. Flight instrumentation and laboratory meters developed to obtain information about the ionized air are described in Section III. Section IV contains a summary of this paper.

II. DISCUSSION OF PLASMA SHEATH [1-7]

In order to circumvent or to find solutions for the problems (e.g., telemetry blackout and enhanced radar cross section) and exploit the opportunities (e.g., magnetoaerodynamic attitude control or MHD power generation during reentry), detailed knowledge of the ionized air forming the plasma sheath is essential. Information can be obtained from calculations, but in order to proceed with the calculations, idealizations and simplification are often necessary. Experiments in hypersonic facilities yield useful information; however, it is difficult to duplicate all the similarity parameters In-flight measurements can be used to provide valuable guides for additional theoretical and experimental work and as criteria to indicate where the calculations are sound and where important physical phenomena have been omitted.

In order to design instruments to measure a property of the plasma sheath it is necessary to know approximately the range of values that will be encountered during reentry. It is necessary to know the correct gain for the amplifiers! Although the information presented in this section was initially obtained to answer the obvious questions of amplifier gain and instrument design, it is of sufficient general interest to warrant inclusion here.

A. Parameters Influencing the Plasma Sheath

The trajectory, or more specifically the altitude and Mach number of the vehicle, has a pronounced influence on the plasma sheath. Table I, which is intended to demonstrate that increased velocity compounds the difficulties with electromagnetic wave propagation, lists typical values of the electron density, N_e, for equilibrium air behind a normal shock.

Table 1. Electron Densities for Different Trajectories

Trajectory	Typical Velocity ft/sec	Electron Density, cm^{-3}	
		200 000 ft alt	300 000 ft alt
Suborbital IRBM	15 100	7×10^{12}	6×10^{10}
Suborbital ICBM	23 200	8×10^{13}	8×10^{11}
Orbital	25 600	2×10^{14}	3×10^{12}
Superorbital (parabolic)	36 700	3×10^{16}	5×10^{14}

Body shape also influences the plasma sheath. Simple axisymmetric bodies are usually categorized as blunt- or sharp-nosed, depending on whether or not the bow shock wave is attached; however, for the purposes of plasma sheath analysis, these bodies are differentiated by the manner in which their sheath properties are determined. Thus, a blunt-nosed body is one whose sheath properties are determined by air that has passed through a normal or nearly normal shock wave. A sharp-nosed body is one whose sheath properties are determined by the viscous dissipation in the boundary layer, which on a sharp-nosed vehicle is supplied with air that has passed through a weak oblique shock.

There is also an intermediate category of vehicle that may be described as slightly blunted. The boundary layer on the forward part of a slightly-blunted vehicle is fed by high-entropy gases from the nose. At some point along the vehicle, the high-entropy flow is absorbed by the boundary layer; downstream from that point the boundary layer feeds on air that has been processed by an oblique shock.

The spatial distribution of temperature and electron density normal to the surface obviously depends on body bluntness. There are, of course, more complex body shapes, especially for manned reentry vehicles, aerospace planes, and other lifting bodies.

Another factor determining the properties of the plasma sheath is the ablation material. Vaporization and injection of the ablation material has a fluid mechanical effect on the boundary layer. Impurities in the ablator may seed the boundary layer and increase N_e. Ablation products influence the chemistry of the high-temperature air by altering compositions and electron densities. An additional degree of complexity is thus added to the plasma sheath.

B. Parameters Characterizing the Plasma Sheath

When a macroscopic approach is used to analyze wave propagation,[8] the plasma is characterized by its electrical permittivity, ϵ, and an electrical conductivity, σ. Attenuation and phase shift can be calculated if these are known.

In terms of microscopic plasma variables, ϵ and σ are functions of the plasma frequency, ω_p (or N_e), and the electron collision frequency, ν. In the presence of magnetic fields the ratio of electron cyclotron frequency to collision frequency may be of importance.

Spatial distribution of ϵ and σ, which is defined both as the profiles normal and tangential to the vehicle surface, is required information for the analysis of wave propagation.[9, 10] The model of a plasma filling a semi-infinite half space is inadequate for obtaining realistic predictions about the plasma sheath.

Table 2 contains information concerning the plasma sheath surrounding a sharp cone. The quantity $\omega_c/\nu B$ determines the strength of magnetic field required to make ω_c/ν equal to unity. This is the strength of magnetic field required to make the plasma behave as an anisotropic medium. For example, in the flank region at 150 000 feet a magnetic field of 157 gauss gives $\omega_c/\nu = 1$. The dc electrical conductivity, equal to $\omega_p^2 \epsilon_o/\nu$, has been calculated. The plasma sheath thickness δ has been taken as being equal to the boundary-layer thickness. In Table 2, δ is for a station 3 ft from the nose.

Table 2. Data for Plasma Sheath on Sharp Cone

Altitude ft	$\omega_c/\nu B$ per gauss	ω_p rad/sec	ν collision/sec	σ mho/m	u m/sec	σu mho/sec	δ cm	N_e cm^{-3}
Stagnation Region[a]								
250	8.8×10^{-3}	1.77×10^{11}	2×10^{9}	140	---	---	---	10^{13}
200	1.25×10^{-3}	5.22×10^{11}	1.41×10^{10}	170	---	---	---	9×10^{13}
150	2.3×10^{-4}	1.51×10^{12}	7.6×10^{10}	270	---	---	---	7×10^{14}
100	3.2×10^{-5}	4.97×10^{12}	5.6×10^{11}	390	---	---	---	8×10^{15}
50	5.5×10^{-6}	4.46×10^{12}	3.2×10^{12}	55	---	---	---	8×10^{15}
Flank Region[a]								
250	0.28	3×10^{9}	6.3×10^{7}	1.4	3500	4900	5	3×10^{9}
200	0.0354	10^{10}	5×10^{8}	1.8	3600	6500	1.5	3×10^{10}
150	6.4×10^{-3}	3×10^{10}	2.75×10^{9}	2.4	3600	8600	0.6	3×10^{11}
100	8.4×10^{-4}	7×10^{10}	2.1×10^{10}	2.3	3500	8100	0.2	1.6×10^{12}
50	1.3×10^{-4}	4.3×10^{10}	1.3×10^{11}	0.12	2800	340	0.08	6×10^{11}

[a]The data are for a semivertex angle of 10 deg, a wall temperature of 2000°K, and an ICBM trajectory with a velocity of 23 500 ft/sec at 150 000 ft alt. The data were calculated using the information from Dix.[4]

The instruments described in the following section measure σu. Hence σu has been calculated using as an estimate $u = u_\infty/2$. One advantage of an instrument that responds to σu is the relatively small change in this quantity with altitude. In the altitude range 250 000 to 100 000 ft, σu varies by less than a factor of 2, whereas N_e changes by a factor of 500. Instruments responding to N_e must have a wide dynamic range. The reason the σ does not change appreciably is that increases in N_e are compensated for by increases in ν.

In contrast to sharp-nosed vehicles, values of σu as high as 5×10^5 mho/sec may be observed in the flank region of blunt-nosed vehicles. This is 100 times larger than for a sharp-nosed vehicle. As a consequence, measurements of the plasma sheath on a sharp-nosed vehicle are significantly more difficult.

III. FLIGHT INSTRUMENTATION DEVELOPED AT PLASMA RESEARCH LABORATORY

Several instruments for measuring plasma sheath properties, which are in various stages of development at the Plasma Research Laboratory, will be described in this section. The first instruments described--three average σu meters and a σu profile instrument--have been flown or are soon to fly. The MHD flow angle indicator, the velocity meter, and the turbulence indicator have been tested in the laboratory. An instrument for the measurement of electron collision frequency has been theoretically analyzed but has not yet been tested in the laboratory. These instruments may be used to measure not only the reentry plasma sheath but also other high-speed ionized-gas flows, including rocket exhausts, MHD generators, and arc plasma jets.

A. Relation of Signal to Flow Properties

In previous publications[1, 11] the signal, which is the voltage induced in the sensing coil, was analyzed in detail. The analysis will be briefly reviewed here.

Consider a coil arrangement consisting of a sensing coil located between two primary coils as shown in Fig. 1. The primary coils are driven at audio frequencies and provide a magnetic field $\vec{B}$ that penetrates into the plasma flowing at velocity $\vec{u}$. Currents, $\vec{J}$, are induced as a result of the motion of the conductor through the magnetic field. The induced magnetic field $\vec{B}_i$, which fluctuates at the frequency of $\vec{B}$, links with the sensing coil that has a voltage e. The currents $\vec{J}$ are equal to $\sigma(\vec{E} + \vec{u} \times \vec{B})$. The electrical conductivity σ is the dc value and for ionized gases equals $\omega_p^2 \epsilon_o / \nu$. It can be shown[2, 12] that, for the two-dimensional case, $\vec{E}$ is zero, and for oblong primary coils (long dimension in the z-direction), $\vec{E}$ is negligible. The voltage in the sensing coil is

$$e = -\frac{NA\mu_o}{4\pi} \frac{\partial}{\partial t} \int_V \frac{\sigma(\vec{u} \times \vec{B}) \times \vec{r}}{r^3} \cdot \vec{n}\, dV - N \frac{\partial}{\partial t} \int \vec{B} \cdot \vec{n}\, dA \quad . \qquad (1)$$

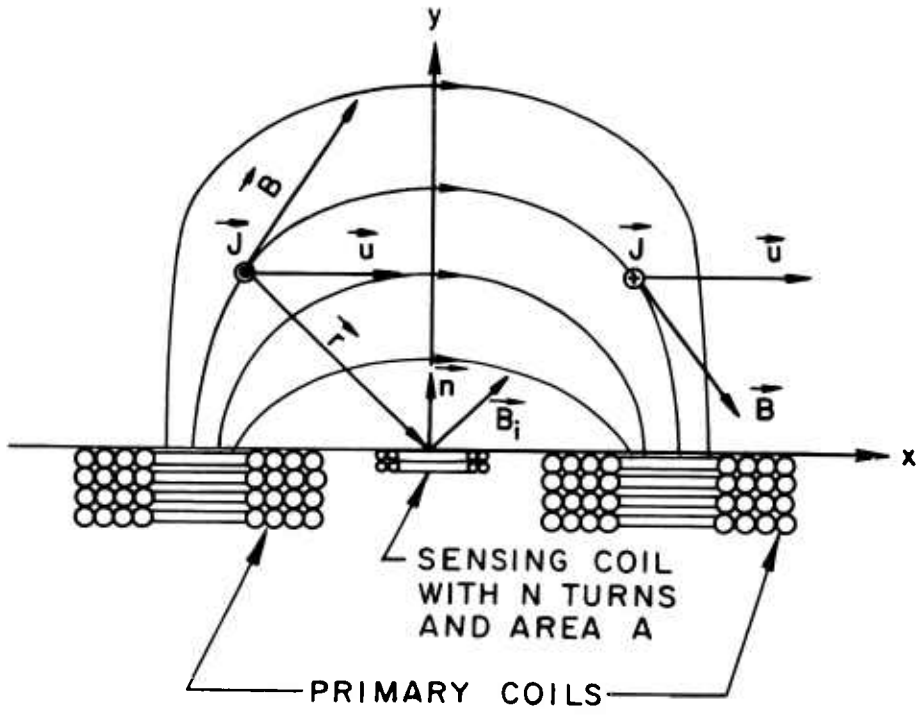

z - AXIS IS NORMAL TO AND OUT OF THE PLANE OF THE PAPER

Fig. 1. Transducer Coil Arrangement

An emf is induced in the sensing coil by the time rate of change of normal component of B_i.

The second integral represents the primary field that links the sensing coil; it is an unwanted voltage and is termed the null signal. By careful balance of the primary field this signal can either be eliminated or made negligibly small. Manipulation of the vectors as indicated in the first integral leads to

$$e = \frac{NA\mu_o\omega}{4\pi} \int_x \int_y \int_z \frac{\sigma(y)u(y)xB_y(x,y,z)}{r^3} \, dx \, dy \, dz \quad , \tag{2}$$

which can be rewritten as

$$e = \int_y \sigma u K \, dy \quad , \tag{3}$$

where

$$K(y) = \frac{NA\mu_o\omega}{4\pi} \int_x \int_z \frac{xB_y(x,y,z)}{r^3} \, dx \, dz \quad . \tag{4}$$

The function K(y) is known as the influence function and can be readily measured in the laboratory.[11] The influence function equals the signal that would result from a unit layer of conducting material with unit conductivity moving at unit velocity and located at distance y.

B. Average σu Transducers

A transducer with a single influence function and hence one signal yields a measurement of the average value of σu as given by

$$\overline{\sigma u} = \frac{e}{\int K \, dy} \tag{5}$$

An average σu transducer was flown successfully aboard a reentry vehicle. This transducer and others will now be discussed.

1. Flight on RVX-2A

An instrument[12] using a transducer geometry similar to that shown in Fig. 1 was flown on board the RVX-2A, a sphere-cone reentry vehicle. This reentry vehicle (R/V) followed a typical ICBM trajectory. Figure 2 shows the location of the transducer on the R/V and the geometrical relation of the flow field to the applied magnetic field. Figure 3 shows the results of the measurement.

The upper curve in Fig. 3 is a plot of the angle of attack of the R/V as a function of time. Also indicated are the periods of fade and blackout of the telemetry. The lower solid curve shows $\overline{\sigma u}$ as a function of time; $\overline{\sigma u}$ was obtained from the flight measurements of e, laboratory measurements of $\int K\, dy$, and Eq. (5). The electrical conductivity behind a normal shock was calculated for the RVX-2A trajectory. Results of the calculations for σ, based on the method outlined by Meyer,[13] are shown by the dashed curve, with values for mho/m, on the right-hand side of the lower graph in Fig. 3.

Observe that the meter signal follows the oscillation of the angle of attack; i.e., a local minimum of the signal corresponds to zero angle of attack. At time A (Fig. 3) the angle of attack is zero, and $\overline{\sigma u}$ is at a minimum. At time B the angle of attack is at its peak value, and $\overline{\sigma u}$ has increased to a local maximum. This fact suggested the instrument described in Section D.

2. Axisymmetric Transducer Geometry[14-16]

Aerodynamic stability requires the center of gravity of the vehicle to be in front of the center of pressure. Conical reentry vehicles frequently require dense ballast placed far forward to achieve this condition. The ballast replaces a part of the payload. A transducer has been developed that serves two functions: it provides measurement of an average value of σu, and its weight serves as ballast. Figure 4 shows the coil arrangement, which has been tested in an arc jet. Analysis shows that most of the signal is due to the induced currents in a narrow region of the plasma flow concentric with the sensing coil. Two reasons account for this. First, the magnetic coupling

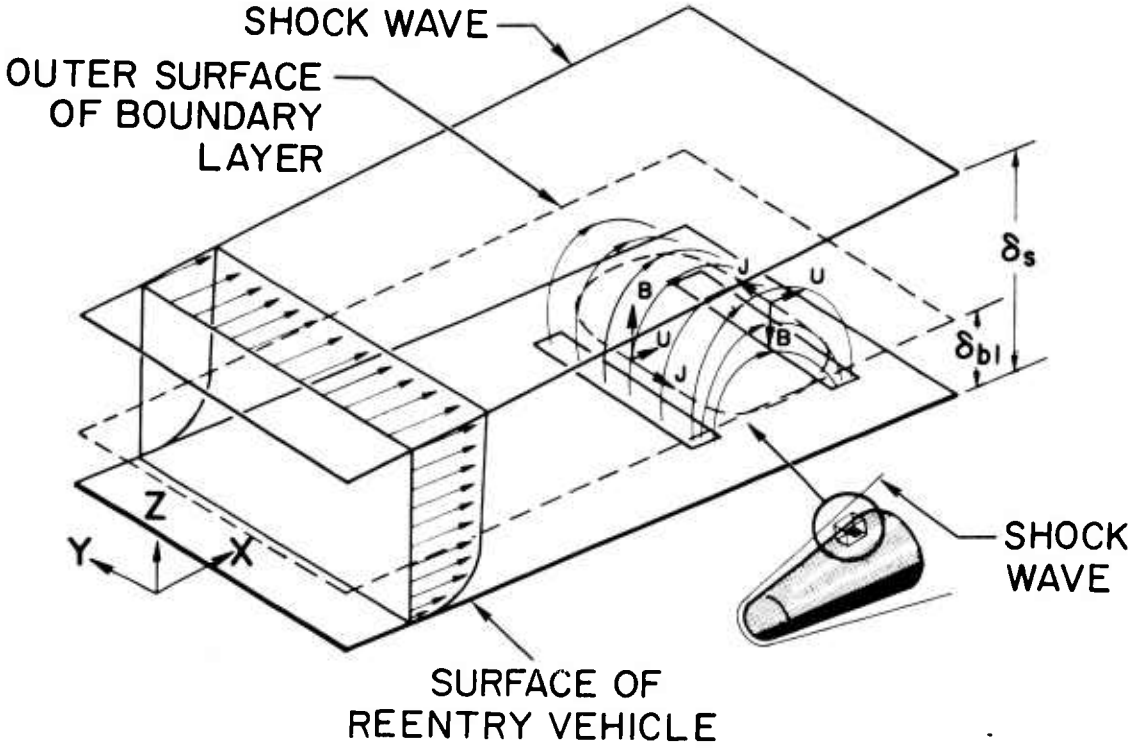

Fig. 2. Flow Field and Location of Transducer on Reentry Vehicle

The coils of the conductivity meter are located well aft on the reentry vehicle. The flow of conducting gas u interacts with the magnetic field B to provide a current density i.

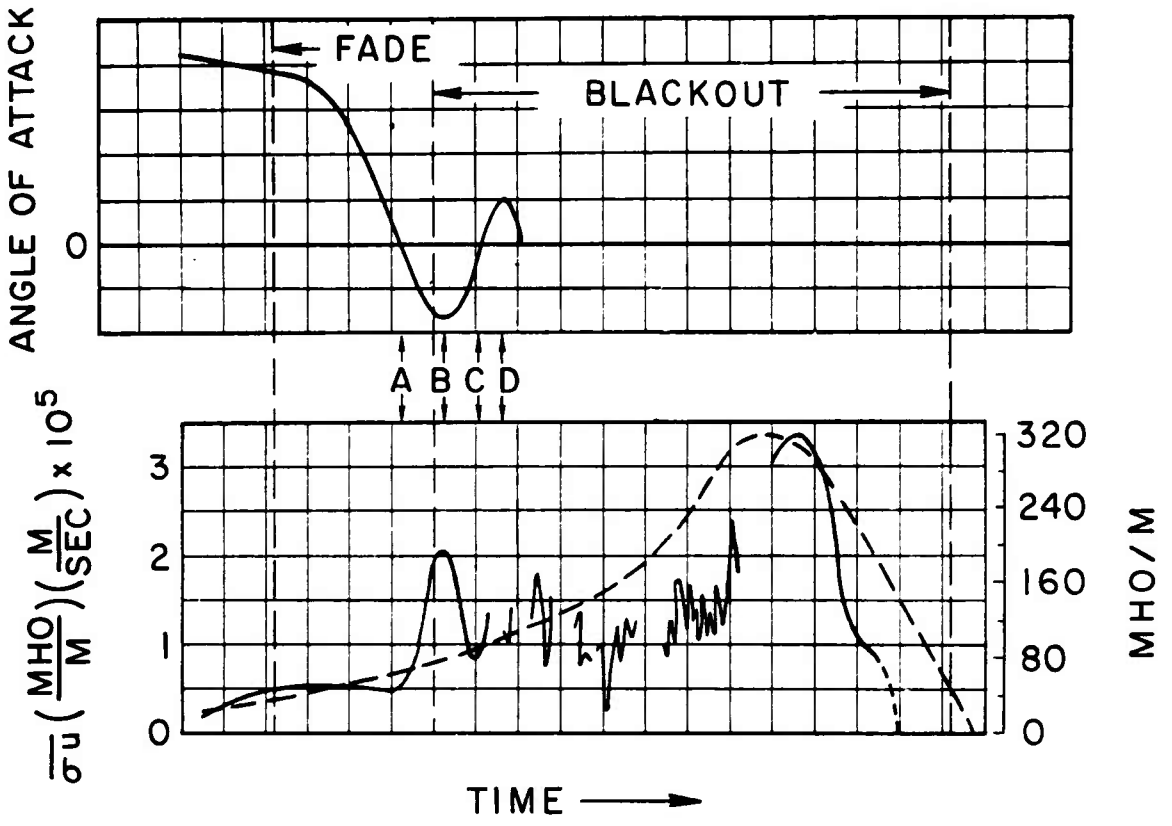

Fig. 3. Observed Value of $\overline{\sigma u}$ and the Angle of Attack of the Reentry Vehicle

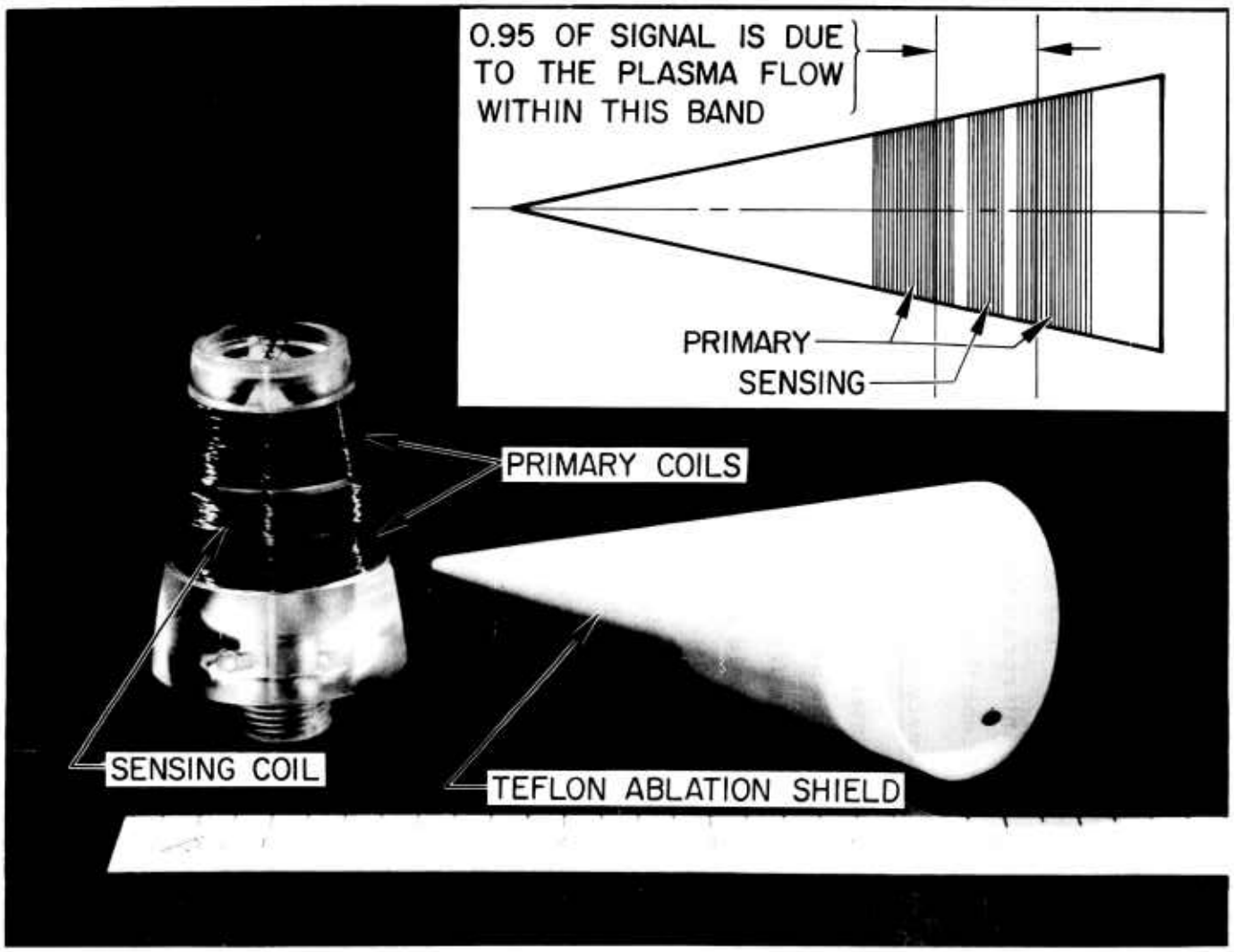

Fig. 4. Average σu Transducer Geometry Readily Adaptable to Cone Designs

between the sensing coil and the current rings in the gas falls off sharply as the separation between the two increases. Second, the applied magnetic field, which drives the currents, falls off rapidly with distance from the sensing coil. For the geometry shown in Fig. 4, 95 percent of the signal is due to the currents within a region in the gas twice the width of the sensing coil (see the inset in Fig. 4). This means that the plasma flow is sampled in the vicinity of the sensing coil, and interpretation of the signal is more meaningful since only a localized region contributes to the signal.

3. Transducer Using Permanent Magnets[17]

When the instrumentation program[2] was first initiated at the Plasma Research Laboratory it was necessary to decide whether to use a dc or an ac applied magnetic field. The first instruments developed used ac. However it is obvious that the induced field B_i exists with a dc primary field. In order to measure σu with a thick metallic skin between the conducting flow and the transducer, a dc meter is essential. If an ac method is attempted, eddy currents in the skin attenuate both the applied magnetic field and the induced magnetic field.

The earth's magnetic field is approximately 500 milligauss. For one application aboard a reentry vehicle the calculated B_i varied between 1 and 10 milligauss. Hence cancellation of the earth's magnetic field is necessary. One method of cancellation is to use two magnetic detectors whose outputs are sensed differentially such that the signal due to earth's magnetic field cancels, whereas the signal due to plasma flow adds. Figure 5 schematically depicts one arrangement. Figure 6 is a photograph of the flight instrumentation package.

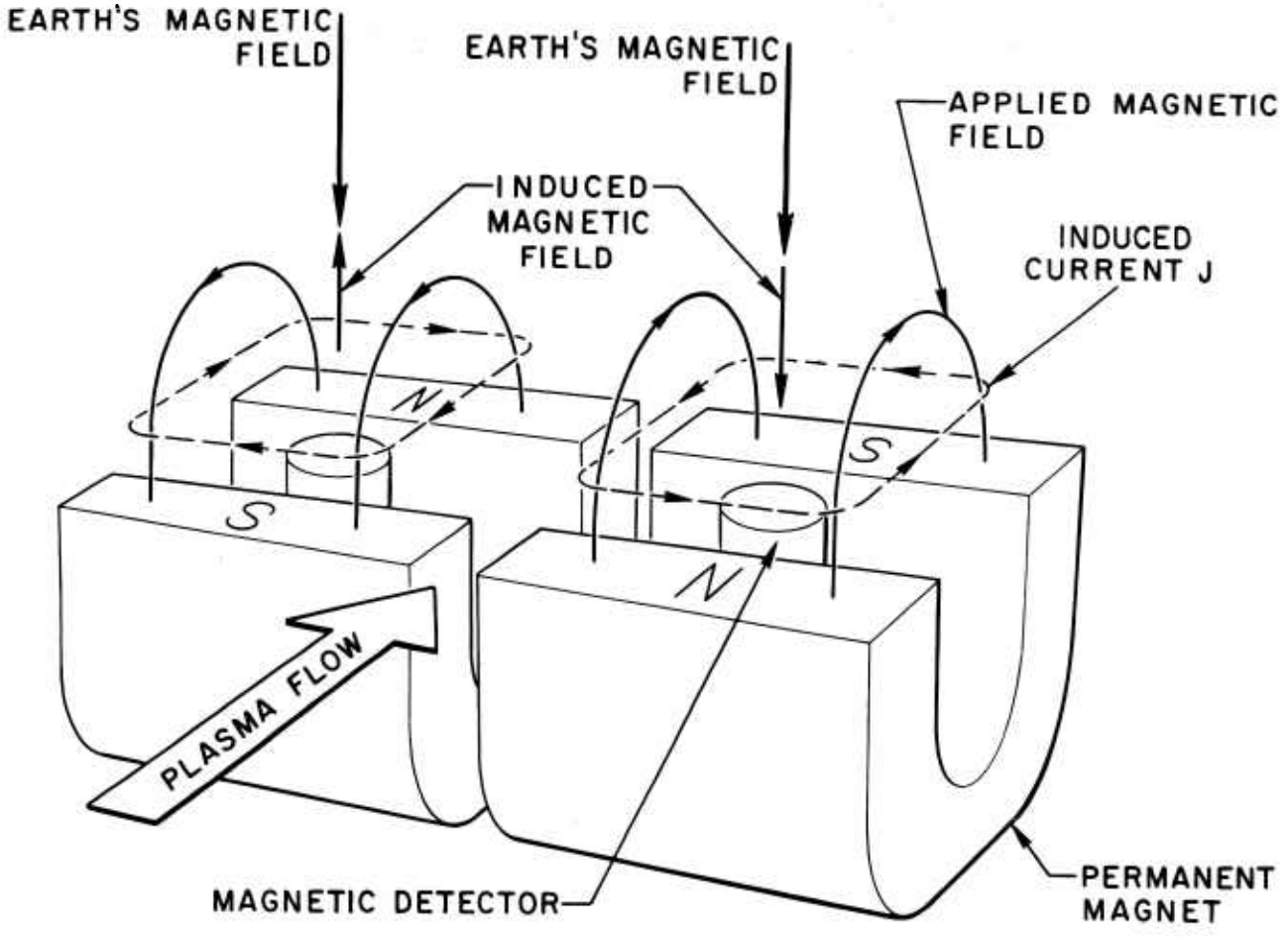

Fig. 5. Cancellation of Earth's Magnetic Field and Addition of Induced Magnetic Field due to Plasma Flow

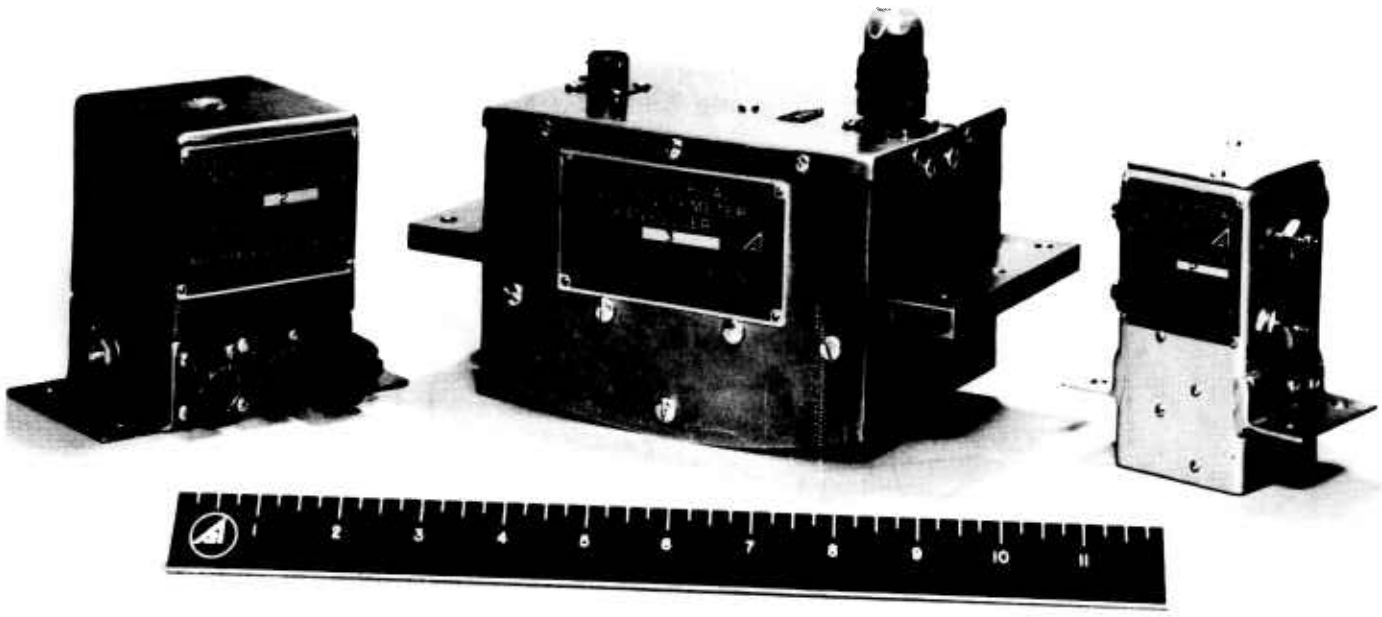

Fig. 6. Flight Instrument to Measure $\overline{\sigma u}$. Transducer, 8 lb; Electronics Box, 2.5 lb; Compensation Box, 1 lb

C. Conductivity/Velocity Profile Meter[1,11]

If transducers with different magnetic field geometries are used, the flow of ionized gas can be sampled differently. Each geometry provides a different signal given by

$$e_i = \int_{\substack{\text{ablation} \\ \text{surface}}}^{\text{shock wave}} \sigma u K_i \, dy \tag{6}$$

where the subscript i identifies the different signals. The K_i are measured in the laboratory; the e_i are measured in flight. Distinctly different K_i can be obtained by changing the primary magnetic field geometry and by altering the geometrical relation between the induced magnetic field and the sensing coils.

From this information the σu profile can be calculated. One procedure is to divide the integration interval into discrete intervals Δy_j, which may be of unequal length. Having chosen the Δy_j, the corresponding $(\sigma u)_j$ values can be determined as shown in Fig. 7. For the case illustrated in Fig. 7, a five-signal transducer is required. A three-signal transducer is shown in Fig. 8. Other geometries, including a nine-signal transducer, have been considered and are discussed in Refs. 1 and 11.

The transducer illustrated in Fig. 8 is designed to sample the plasma flow in different ways by having different scale primary fields. A plasma layer of Δy thickness appears to the small primary coil to be $\Delta y/R = 1$ in thickness and to be centered at $y/R = 2$. The same plasma layer appears to the large primary coil to be $\Delta y/R = 1/3$ in thickness and to be centered at $y/R = 2/3$. The plasma layer is measured by use of different portions of the influence function.

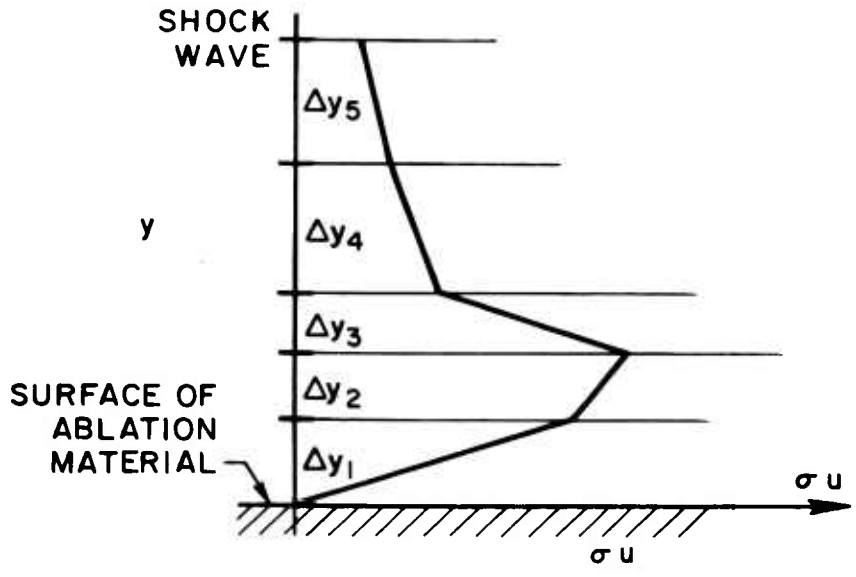

Fig. 7. Illustration of the Results of a Calculation of σu Profile

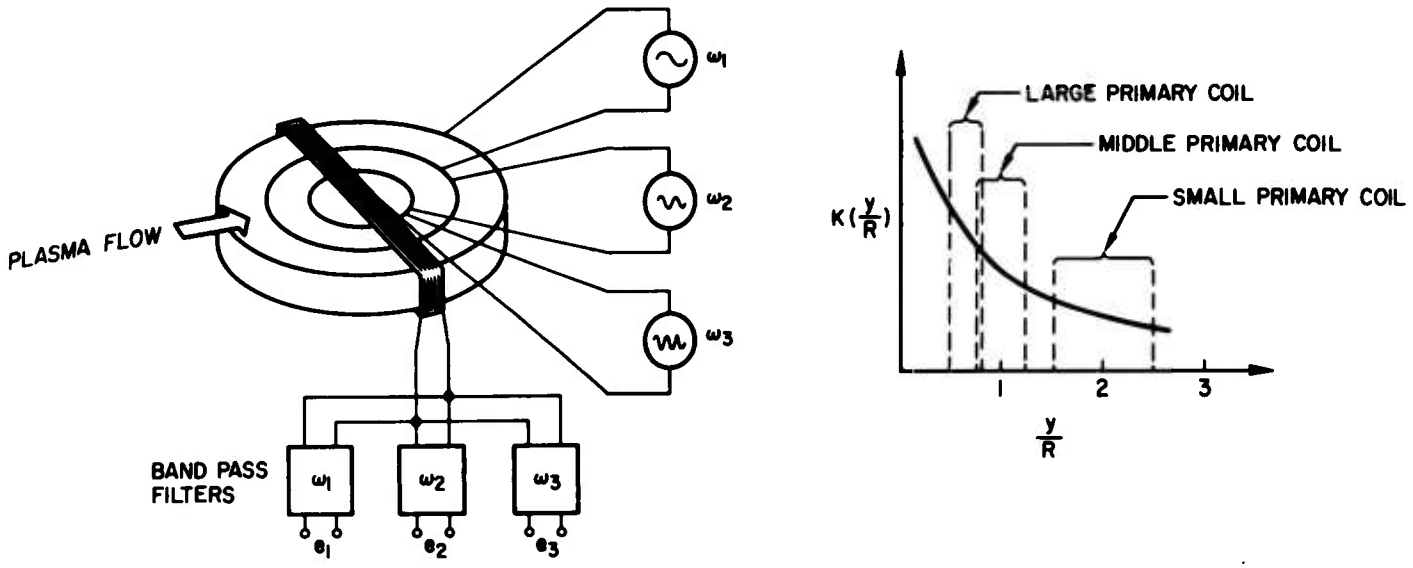

Fig. 8. A Coil Geometry Providing Three Different Scale Primary Fields

Using knowledge of e_1, e_2, e_3 and the influence functions K_1, K_2, and K_3 from the system shown in Fig. 8, the profile of a spinning graphite disc was calculated. A comparison of the actual and measured profiles is shown in Fig. 9. Three different experiments are plotted, with the disc located at 0.5, 1.0, and 2.0 inches from the transducer. The influence function for the smallest primary coil has been plotted in the bottom graph. The error in predicting the disc thickness, when the disc was 2 inches from the transducer, is due to the fact the meter is not sensitive beyond about 3 inches.

A MHD profile meter[18] has been built for flight aboard reentry vehicles. Figure 10 is a photograph of the instrument, which provides four continuous samples of the flow. A similar instrument is being developed for flight on board the Low Observable Reentry Vehicle (LORV).

D. Flow Angle Indicator[19]

The instruments described in this and the following two sections have been tested in the laboratory but have not been developed as flight instrumentation.

Using the magnetohydrodynamic (MHD) flow angle indicator is analogous to using two total head tubes displaced at a small angle to measure flow angles. When the pressure in each tube is equal, the bisector of the tube angle is parallel to the flow. The MHD flow angle indicator is shown in Fig. 11. The transducer is not rotated to give equal signals, but the ratio of signal strength is used to calculate the flow angle. The equation relating signal ratio R to flow angle θ is

$$\theta = \arctan\left(\frac{1 - R}{1 + R} \frac{1}{\tan \alpha}\right) \tag{7}$$

The symbols are defined in Fig. 11. The angle α measures the location of the sensing coils relative to the reference axis. When the plasma flow, which is above and parallel to the plane of the paper, deviates by an angle θ from the

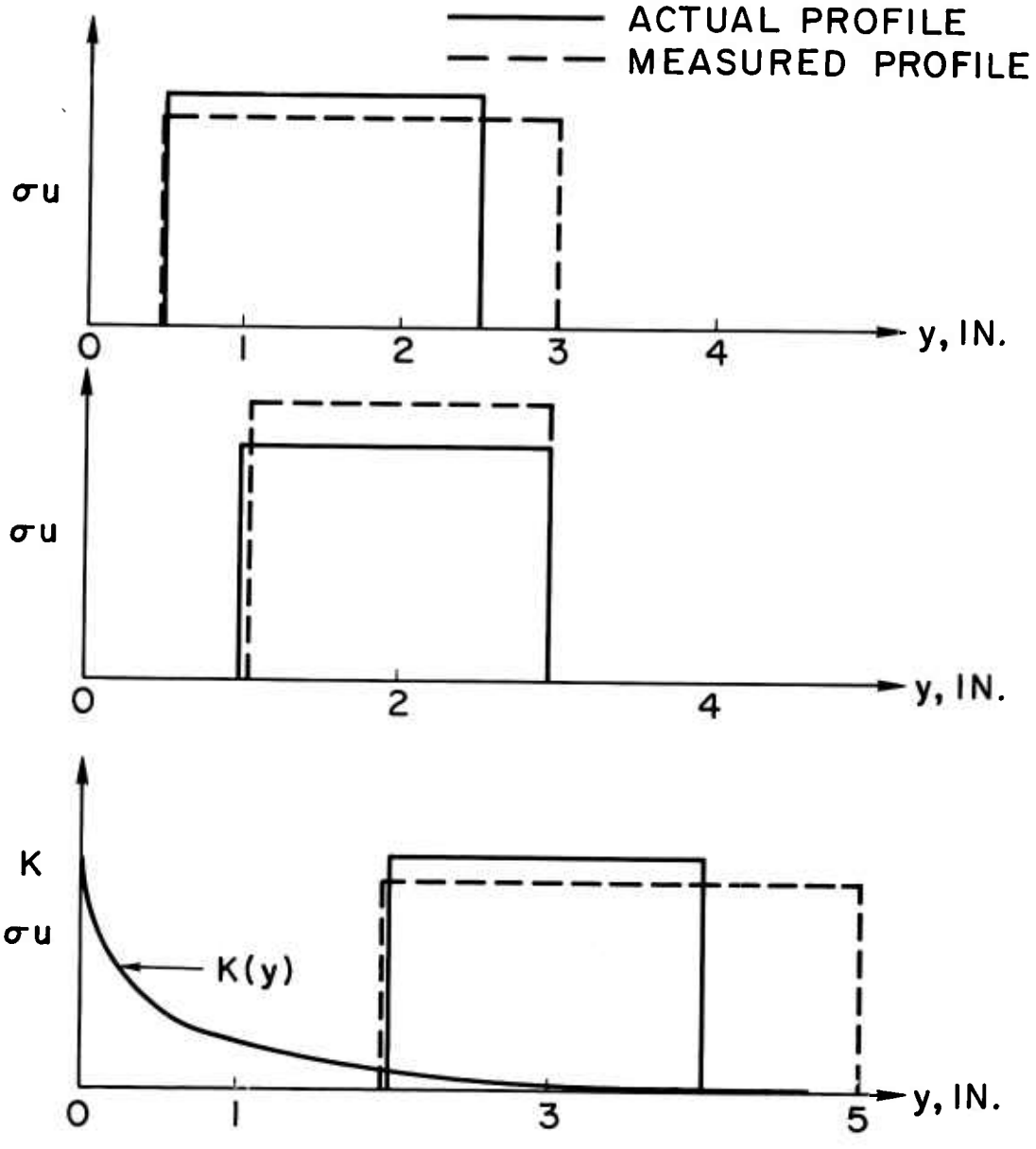

Fig. 9. Comparison of Actual and Measured Profiles

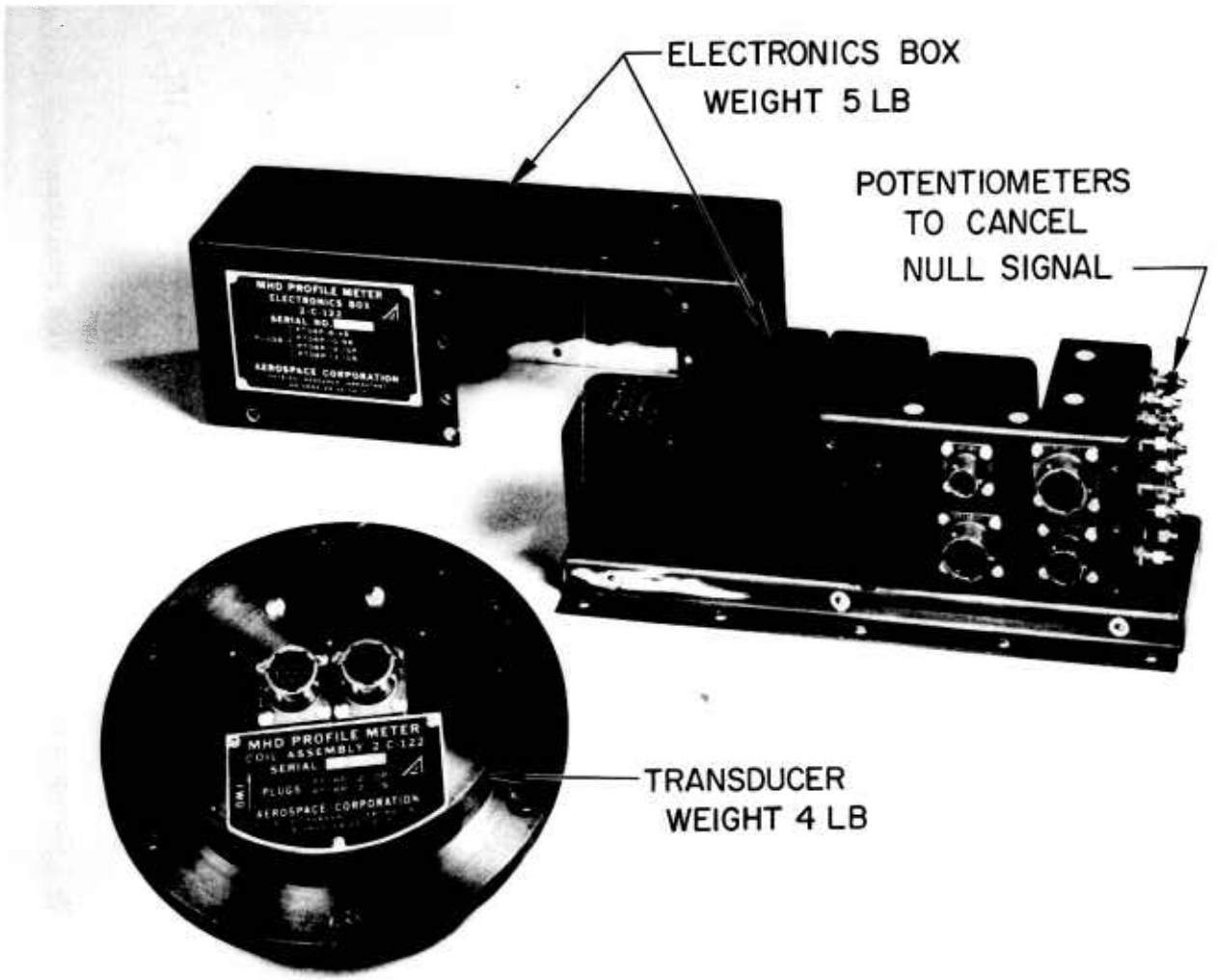

Fig. 10. MHD Electrical Conductivity/Velocity Profile Meter

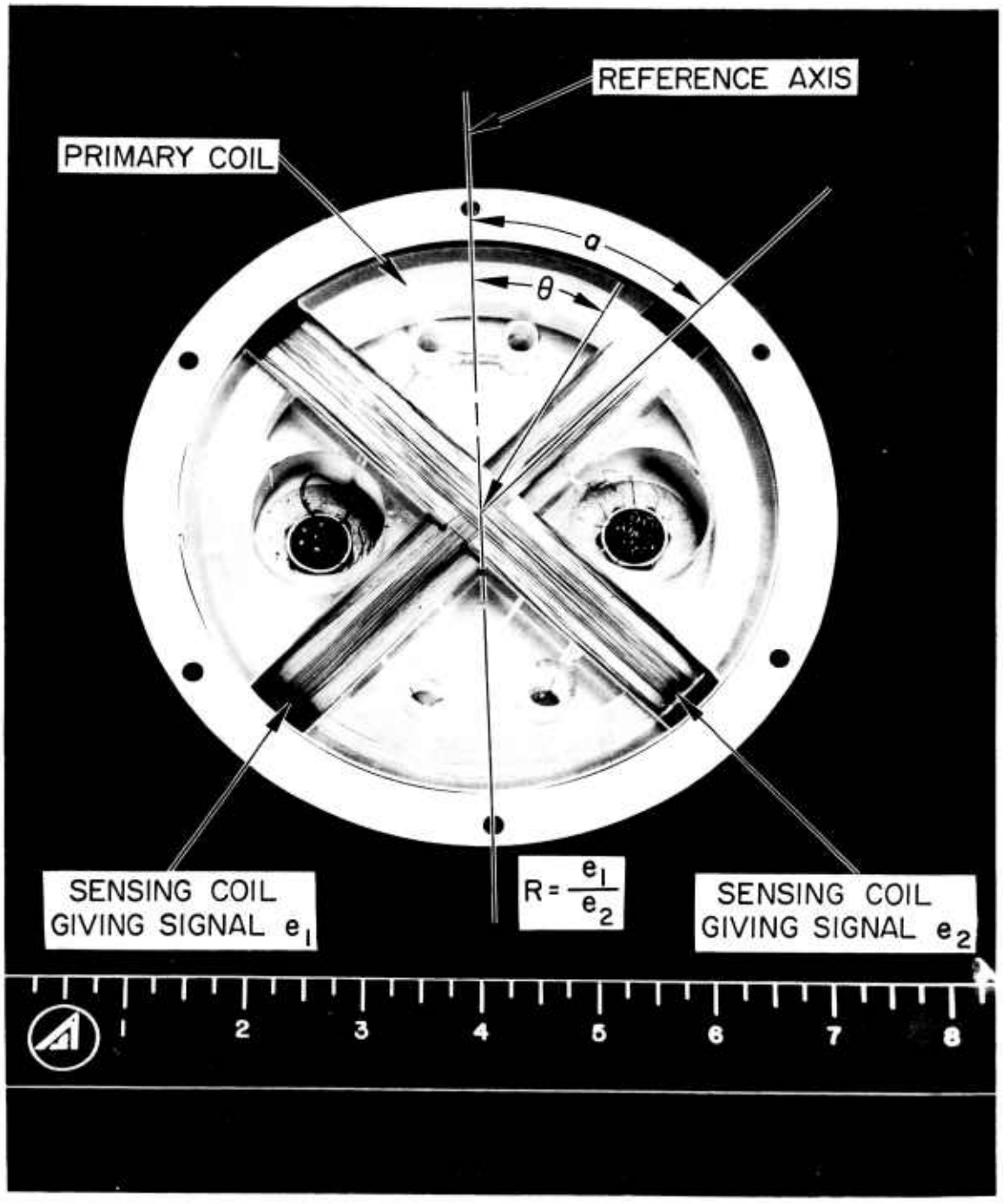

Fig. 11. Crossed Sensing Coil Geometry

reference axis, sensing coil 2 has a larger signal than sensing coil 1. Equation (7) gives θ as a function of the signal ratio R and α. The transducer can yield the local flow angle θ without knowledge of σ or u of the ionized gas. However, if e_1 and e_2 are measured separately and the transducer is calibrated, simultaneous measurements of σu and θ are obtained.

Two different configurations have been built and tested: one is shown in Fig. 11; the other is described in Ref. 19. The accuracy of the flow angle measurement is 1 deg ±5% for -45 deg < θ < 45 deg. (For an angle of 40 deg, the error may be ±3%.) For bounded θ, the α can be adjusted to give optimum performance.

E. Average Electron Collision Frequency[20]

A scalar electrical conductivity has been assumed in the previous sections. If a sufficiently large magnetic field is applied, the σ becomes a tensor. Table 1 gives the value of B required for a ratio of electron cyclotron frequency ω_c to collision frequency ν equal to unity. Equation (1) has been expanded, considering σ to be a tensor. For the coordinate system and coil arrangement shown in Fig. 1, the result is

$$e = -\frac{NA\mu_o}{4\pi}\frac{\partial}{\partial t}\int_V \frac{u\sigma'}{1+\left(\frac{\omega_c}{\nu}\right)^2}\left[\left(\frac{\omega_z\omega_y}{\nu^2}+\frac{\omega_x}{\nu}\right)\left(-\frac{B_z x}{r^3}\right)+\left(1+\frac{\omega_z^2}{\nu^2}\right)\left(\frac{B_y x}{r^3}\right)\right.$$
$$\left.+\left(\frac{\omega_y\omega_x}{\nu^2}-\frac{\omega_z}{\nu}\right)\left(\frac{B_z z}{r^3}\right)-\left(\frac{\omega_x\omega_z}{\nu^2}+\frac{\omega_y}{\nu}\right)\left(\frac{B_y z}{r^3}\right)\right]dV \quad (8)$$

where ω_x, ω_y, and ω_z are the components of ω_c, and σ' equals $\omega_p^2\epsilon_o/\nu$. Fortunately, most of the terms drop out in the integration as a result of symmetry. In final form the equation for the signal voltage is

$$e = -\frac{NA\mu_o}{4\pi}\frac{\partial}{\partial t}\int_V \frac{u\sigma'}{1+\frac{\omega_c^2}{\nu^2}}\frac{B_y x}{r^3}\,dV \quad (9)$$

Note that when $(\omega_c/\nu)^2 << 1$, Eq. (9) reduces to Eq. (2).

An average value of the ratio ω_c/ν can be measured by using an applied magnetic field as illustrated in Fig. 12. When an appropriately strong dc field is applied, the denominator of the integrand in Eq. (9) exceeds unity, decreasing the signal. When the primary coil is excited only with weak ac, the denominator is nearly unity and a signal e_o is measured. An average value of the frequency ratio is given by

$$\left(\frac{\nu}{\omega_c'}\right)_{\text{average}} = \left(\frac{e}{e_o - e}\right)^{1/2} \tag{10}$$

where $\omega_c' = eB_{dc}/m$.

F. Velocity Measurement

An experiment was performed using the coil arrangement shown in Fig. 13 and an arc plasma jet. The primary coils were excited dc and had alternating poles. Emitter followers were used to isolate the sensing coils from the distributed capacitance in the external leads. A flat frequency response from 10 to 100 kc was thus obtained.

Typical traces of the voltage induced in the sensing coils as a result of the plasma jet flowing through the steady applied magnetic field are shown in Fig. 14. Voltages appearing at the upstream and downstream sensing coils are closely correlated. The cross correlation function

$$F(\tau) = \frac{\int e_1(t)e_2(t+\tau)\,dt}{\left(\int e_1^2\,dt\right)^{1/2}\left(\int e_2^2\,dt\right)^{1/2}} \tag{11}$$

was calculated as a function of τ for several oscillograms similar to Fig. 14. Maximum values of F ranged from 0.85 to 0.92.

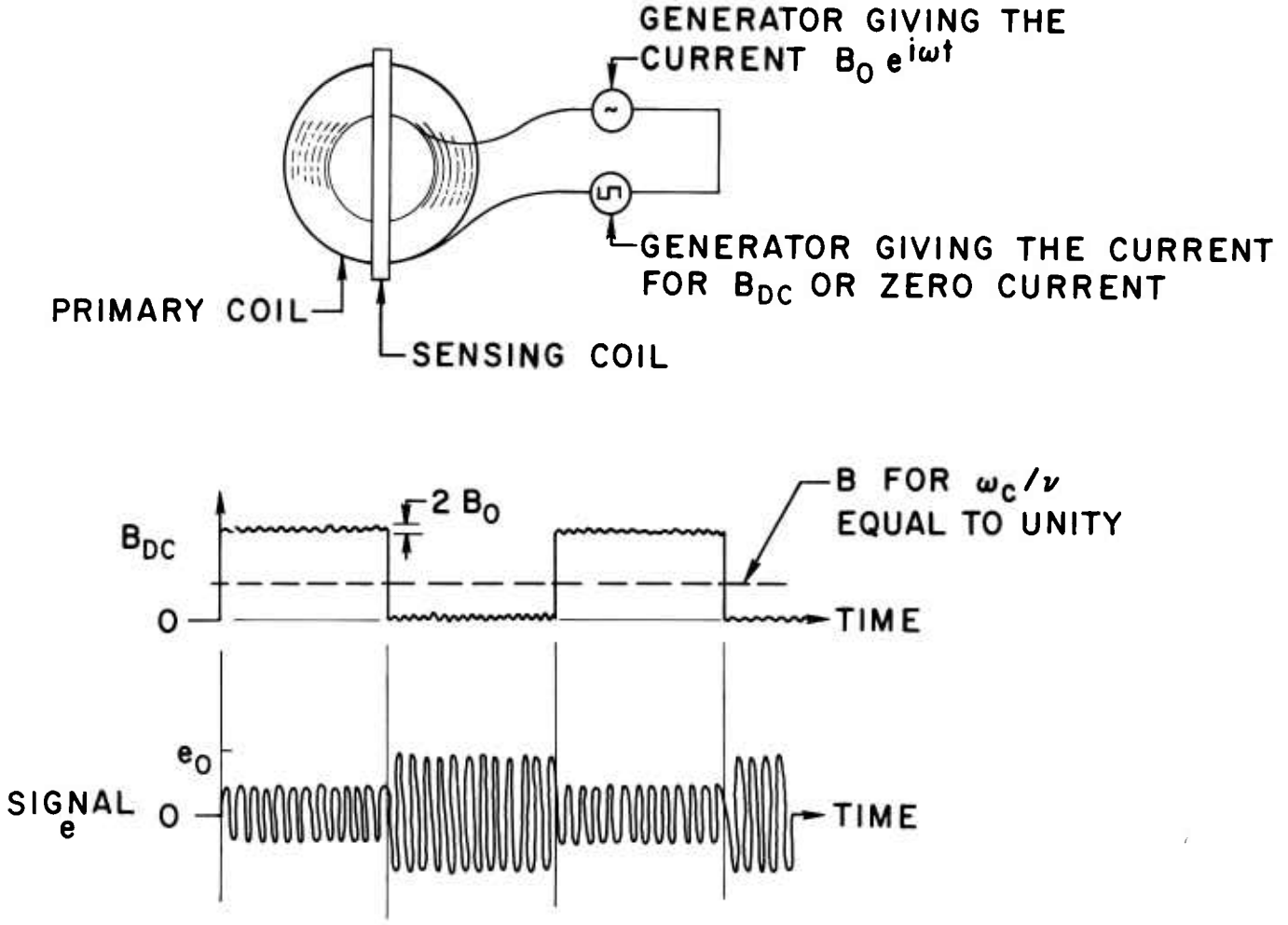

Fig. 12. The Excitation of the Primary Field and the Anticipated Signal

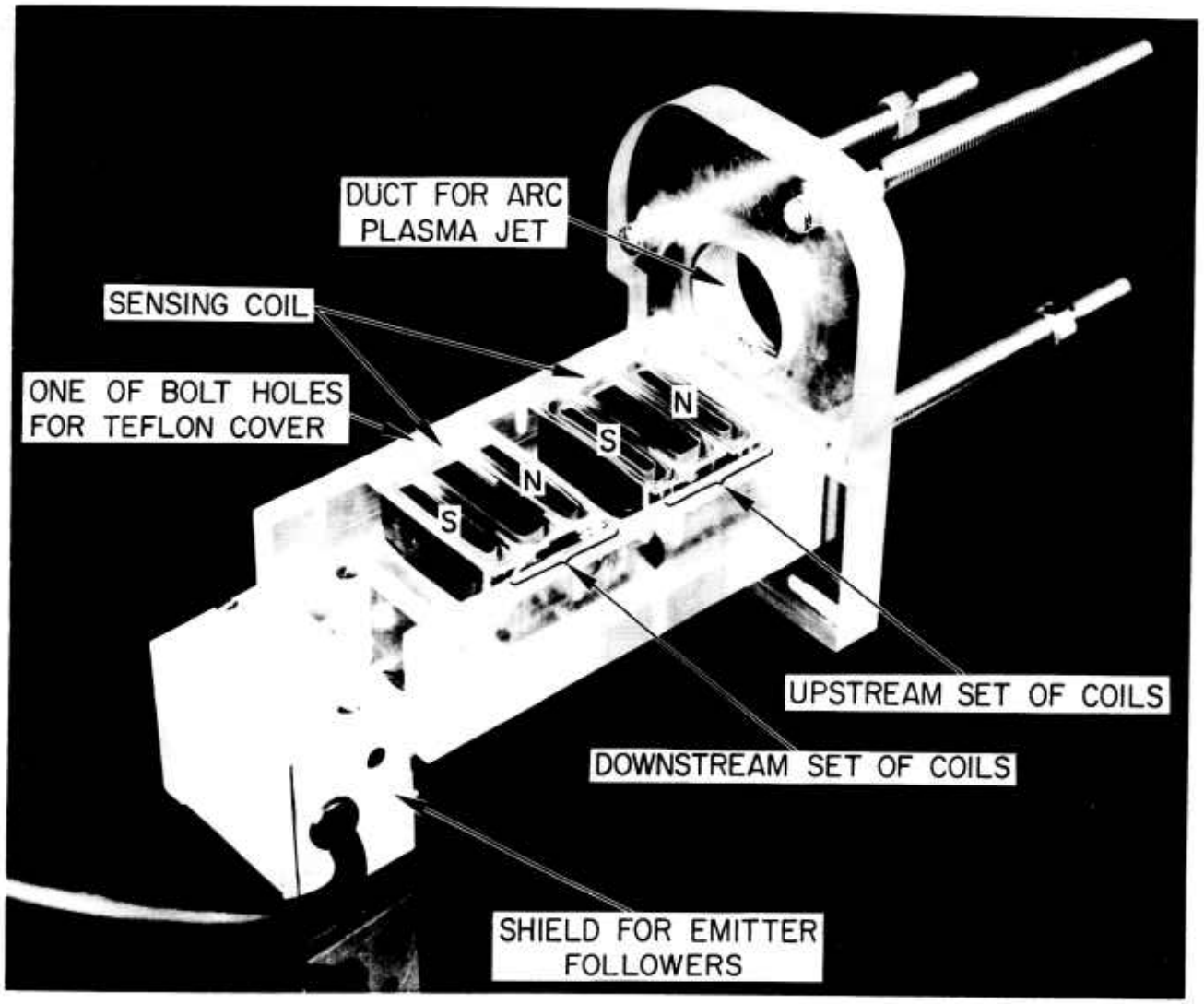

Fig. 13. Velocity and Turbulence Transducer

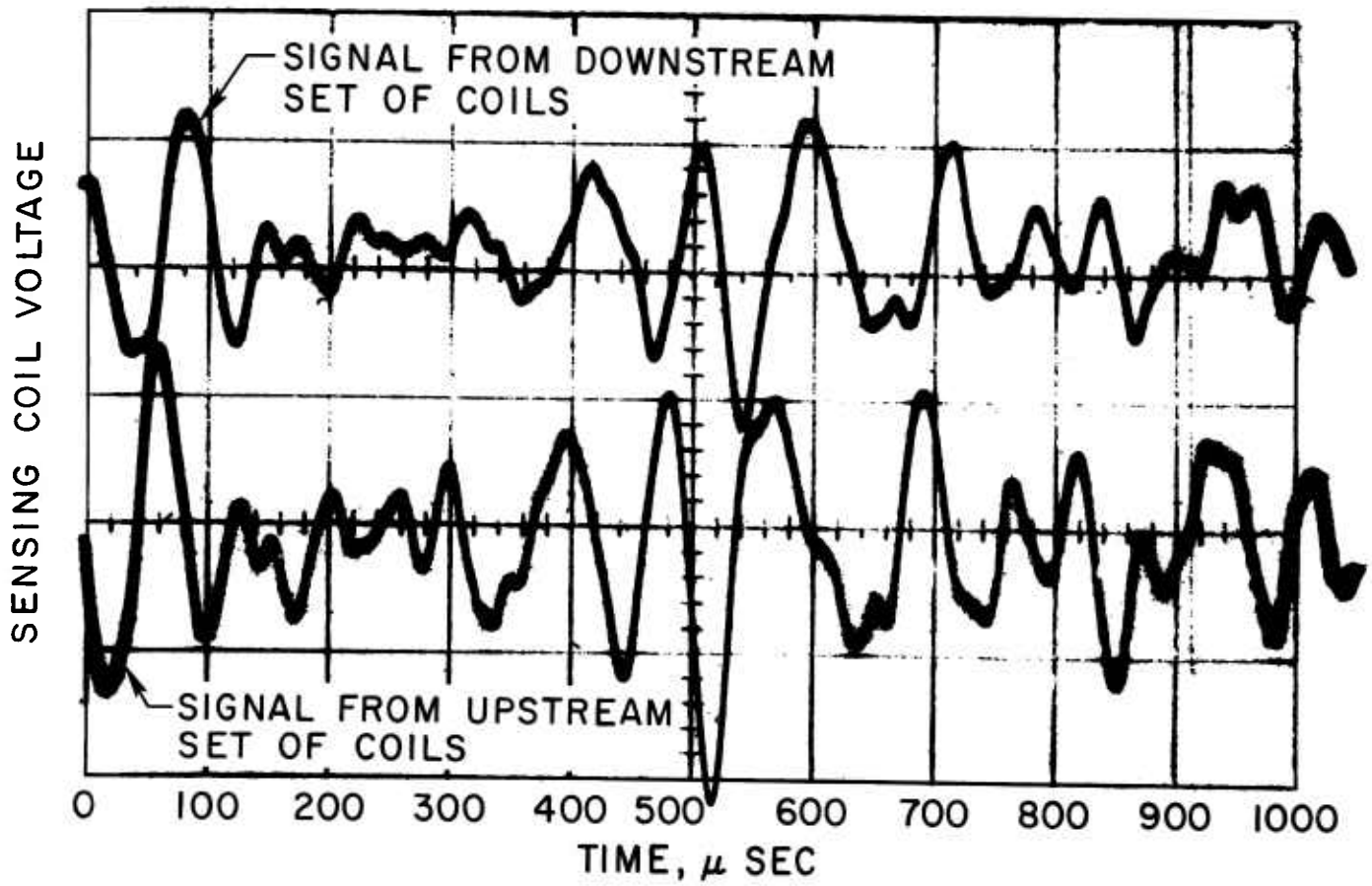

Fig. 14. Typical Signals from Velocity Transducer

For the case shown in Fig. 14 the peak value of F occurred at $\tau = 22$ μsec. The distance between the upstream and downstream coil sets was 7.9 cm giving a velocity of 3600 m/sec.

G. Turbulence Indicator

The preceding experiment is an example of serendipity. The aim was to measure velocity, and an average velocity measurement was obtained; however, it was discovered that additional information about the flow is contained in the noisy signal traces. The amplitude and spectrum of the signals illustrated in Fig. 14 are related to σu fluctuations in the plasma stream.

Although the data obtained await thorough analysis, preliminary observations can be made. The time dependent terms in Eq. (1) are σ and u, and not B. The close correlation between the upstream and downstream signals indicates that the σu fluctuations are convected, with only small changes due to the nonstationary terms. The spectrum is dictated by the response of the transducer to the different scale σu fluctuations. Experiments using wire loops that are moved through the applied magnetic field indicate that only loops in the range 0.5L to 2.0L cause significant signals (L is the length of one complete coil set in the streamwise direction).

The signals were obtained in an arc jet facility. It is not known whether similar fluctuations occur in the plasma sheath surrounding a reentry vehicle. One application of the turbulence indicator would be to detect on a reentry vehicle the transition from laminar to turbulent flow. Since the skin depth at 10 to 100 kc in most metals is very small, the turbulence transducer should be separated from the flow by dielectrics only.

IV. SUMMARY

Several instruments have been developed, which depend for their operation on the interaction of a high speed flow of ionized gas with an applied magnetic field. These meters are admirably suited for reentry experiments because the transducer can be located behind a protective wall and does not require probes that have to be inserted into the plasma.

The average σu meters in two geometrical arrangements have been developed for flight. One σu profile meter has been assembled (Fig. 10) as a flight instrument; another model is under development. Instruments to measure local flow angle (Fig. 11), average flow velocity, and fluctuations (Fig. 13) have been tested in the laboratory. An average electron frequency meter (Fig. 12) has been explored theoretically.

ACKNOWLEDGEMENT

The first in the series of the electrical conductivity/velocity instruments was conceived by R. X. Meyer. His help and encouragement with the development of the other transducers is appreciated.

Frequent discussions with R. Betchov concerning various aspects of the instruments were extremely helpful. In addition he suggested the velocity measurement experiment and helped with the development of the dc version of the average σu transducer.

L. S. G. Kovasznay, consultant to Plasma Research Laboratory, provided new insight into the σu profile meter. He also reviewed the work done on the tensor conductivity (average ν measurement) and made helpful suggestions.

O. L. Gibb assembled, calibrated, and assisted with the design of the transducers. In addition, he is co-inventor of the MHD flow angle indicator. A. Y. Lu translated rough sketches into polished engineering designs. His assistance has been invaluable.

REFERENCES

1. Fuhs, A.E., "A Technique for Obtaining the Velocity-Electrical Conductivity Profile," TDR-594(1215-01)TN-2, Aerospace Corporation, El Segundo, Calif. (30 June 1961); see also Proceedings of the Second Symposium on the Plasma Sheath (Plenum Press, New York, 1962).

2. Fuhs, A.E., "Development of a Device for Measuring Electrical Conductivity of Ionized Air During Reentry," STL/TR-60-0000-09256, Space Technology Labs., Los Angeles (20 September 1960).

3. Rotman, W., and G. Meltz, eds., "Electromagnetic Effects of Reentry, Selected papers from Symposium on the Plasma Sheath: Its Effects on Communication and Detection" in Planetary and Space Science (June 1961), vol. 6.

4. Dix, D.M., "Typical Values of Plasma Parameters Around a Conical Reentry Vehicle," TDR-169(3230-22)TN-1, Aerospace Corporation, El Segundo, Calif. (7 November 1962).

5. Lincoln Lab., Massachusetts Inst. of Tech., "Reentry Physics and Project Press Programs, Semiannual Technical Summary Reports to the Advanced Research Projects Agency," (30 June and 31 December 1960, 30 June and 31 December 1961, 30 June 1962).

6. Huber, P.W., and C.H. Nelson, "Plasma Frequency and Radio Attenuation," paper 61, NASA University Conference on the Science and Technology of Space Exploration (Chicago, 1962), vol. 2, pp. 347-60. (NASA-11)

7. Pippert, G.F., and S. Edelberg, "The Electrical Properties of the Air Around a Reentering Body," IAS paper 61-40, AIAA(IAS), New York (1961).

8. Plugge, R.J., S. Chen, and R.K. Long, "Some Calculations of the Phase Shift and Attenuation Rates of the Hypersonic Plasma Sheath," Report 1021-3, Ohio State Univ. Research Foundation, Columbus (31 January 1961).

9. Albini, F.A., and R.G. Jahn, "Reflection and Transmission of Electromagnetic Waves at Electron Density Gradients," J. Appl. Phys. 32(1), 75-82 (1961).

10. Daiber, J.W., and H.S. Glick, "Plasma Studies in a Shock Tube," AF-1441-A-4, Cornell Aeronautical Lab., Inc., Buffalo (July 1961).

11. Fuhs, A. E., "Additional Comments on a Technique for Obtaining the Electrical Conductivity-Velocity Profile," TDR-930(2230-03)TN-5, Aerospace Corporation, El Segundo, Calif. (22 March 1962); see also Proceedings of Second Symposium on the Plasma Sheath (Plenum Press, New York, 1962).

12. Betchov, R., A. E. Fuhs, R. X. Meyer, and A. B. Schaffer, "Measurement of Electrical Conductivity of Ionized Air During Reentry," TDR-930(2230-03)TR-1, Aerospace Corporation, El Segundo, Calif. (16 January 1962); also Aerospace Eng. 21 (11), 54-55, 68-78 (1962).

13. Meyer, R. X., "The Electrical Conductivity of Air Up to 2400°K," GM-TR-0127-00420, Space Technology Labs., Inc., Los Angeles (26 June 1958).

14. Fuhs, A. E., and O. L. Gibb, "A Velocity-Electrical Conductivity Transducer For Axisymmetric Reentry Vehicles," Technical Documentary Report, Aerospace Corporation, El Segundo, Calif. (To be published).

15. Sheriff, J. A., "The Theory of Electromagnetic Flow Measurement (Cambridge Univ. Press, New York, 1962).

16. Lehde, H., and H. T. Lang, U. S. Patent 2,435,043 (1948).

17. Fuhs, A. E., R. Betchov, O. L. Gibb, and J. R. Abshear, "An Electrical Conductivity-Velocity Instrument Using DC Applied Magnetic Field," Technical Documentary Report, Aerospace Corporation, El Segundo, Calif. (To be published).

18. Fuhs, A. E., and O. L. Gibb, "Magnetohydrodynamic Electrical Conductivity-Velocity Profile Instrument," Technical Documentary Report, Aerospace Corporation, El Segundo, Calif. (To be published).

19. Fuhs, A. E., and O. L. Gibb, "A Magnetohydrodynamic Flow Angle Indicator," TDR-169(3153)TN-4, Aerospace Corporation, El Segundo, Calif. (13 November 1962); also Presented at Fourth Symposium Engineering Aspects of Magnetohydrodynamics, 10-11 April 1963.

20. Fuhs, A. E., "Signal from the Electrical Conductivity/Velocity Meter for Tensor Conductivity," TDR-69(2119)TN-5, Aerospace Corporation, El Segundo, Calif. (22 May 1962).

Aerospace Corporation, El Segundo, California.
FLIGHT INSTRUMENTATION FOR REENTRY PLASMA SHEATH, prepared by Allen E. Fuhs.
12 July 1963. [46]p. incl. illus.
(Report TDR-169(3153-20)TN-1;BSD-TDR-63-124)
(Contract AF 04(695)-169) Unclassified Report

A number of instruments for probing the plasma sheath during reentry are described. The instruments respond to the induced magnetic field produced by the interaction of the ionized gas flowing through an applied magnetic field. Flight models to measure the product of electrical conductivity and velocity, σu, and the σu profile are discussed. In addition analysis and description of laboratory transducers for determining velocity, σu fluctuations, and average electron collision frequency are presented.

UNCLASSIFIED

UNCLASSIFIED

Aerospace Corporation, El Segundo, California.
FLIGHT INSTRUMENTATION FOR REENTRY PLASMA SHEATH, prepared by Allen E. Fuhs.
12 July 1963. [46]p. incl. illus.
(Report TDR-169(3153-20)TN-1;BSD-TDR-63-124)
(Contract AF 04(695)-169) Unclassified Report

A number of instruments for probing the plasma sheath during reentry are described. The instruments respond to the induced magnetic field produced by the interaction of the ionized gas flowing through an applied magnetic field. Flight models to measure the product of electrical conductivity and velocity, σu, and the σu profile are discussed. In addition analysis and description of laboratory transducers for determining velocity, σu fluctuations, and average electron collision frequency are presented.

UNCLASSIFIED

UNCLASSIFIED

Aerospace Corporation, El Segundo, California.
FLIGHT INSTRUMENTATION FOR REENTRY PLASMA SHEATH, prepared by Allen E. Fuhs.
12 July 1963. [46]p. incl. illus.
(Report TDR-169(3153-20)TN-1;BSD-TDR-63-124)
(Contract AF 04(695)-169) Unclassified Report

A number of instruments for probing the plasma sheath during reentry are described. The instruments respond to the induced magnetic field produced by the interaction of the ionized gas flowing through an applied magnetic field. Flight models to measure the product of electrical conductivity and velocity, σu, and the σu profile are discussed. In addition analysis and description of laboratory transducers for determining velocity, σu fluctuations, and average electron collision frequency are presented.

UNCLASSIFIED

UNCLASSIFIED

Aerospace Corporation, El Segundo, California.
FLIGHT INSTRUMENTATION FOR REENTRY PLASMA SHEATH, prepared by Allen E. Fuhs.
12 July 1963. [46]p. incl. illus.
(Report TDR-169(3153-20)TN-1;BSD-TDR-63-124)
(Contract AF 04(695)-169) Unclassified Report

A number of instruments for probing the plasma sheath during reentry are described. The instruments respond to the induced magnetic field produced by the interaction of the ionized gas flowing through an applied magnetic field. Flight models to measure the product of electrical conductivity and velocity, σu, and the σu profile are discussed. In addition analysis and description of laboratory transducers for determining velocity, σu fluctuations, and average electron collision frequency are presented.

UNCLASSIFIED

UNCLASSIFIED

UNCLASSIFIED

UNCLASSIFIED

UNCLASSIFIED

UNCLASSIFIED

UNCLASSIFIED

UNCLASSIFIED

UNCLASSIFIED

UNCLASSIFIED

Aerospace Corporation, El Segundo, California. FLIGHT INSTRUMENTATION FOR REENTRY PLASMA SHEATH, prepared by Allen E. Fuhs. 12 July 1963. [46]p. incl. illus.
(Report TDR-169(3153-20)TN-1; BSD-TDR-63-124)
(Contract AF 04(695)-169) Unclassified Report

A number of instruments for probing the plasma sheath during reentry are described. The instruments respond to the induced magnetic field produced by the interaction of the ionized gas flowing through an applied magnetic field. Flight models to measure the product of electrical conductivity and velocity, σu, and the σu profile are discussed. In addition analysis and description of laboratory transducers for determining velocity, σu fluctuations, and average electron collision frequency are presented.

UNCLASSIFIED

UNCLASSIFIED

Aerospace Corporation, El Segundo, California. FLIGHT INSTRUMENTATION FOR REENTRY PLASMA SHEATH, prepared by Allen E. Fuhs. 12 July 1963. [46]p. incl. illus.
(Report TDR-169(3153-20)TN-1; BSD-TDR-63-124)
(Contract AF 04(695)-169) Unclassified Report

A number of instruments for probing the plasma sheath during reentry are described. The instruments respond to the induced magnetic field produced by the interaction of the ionized gas flowing through an applied magnetic field. Flight models to measure the product of electrical conductivity and velocity, σu, and the σu profile are discussed. In addition analysis and description of laboratory transducers for determining velocity, σu fluctuations, and average electron collision frequency are presented.

UNCLASSIFIED

UNCLASSIFIED

Aerospace Corporation, El Segundo, California. FLIGHT INSTRUMENTATION FOR REENTRY PLASMA SHEATH, prepared by Allen E. Fuhs. 12 July 1963. [46]p. incl. illus.
(Report TDR-169(3153-20)TN-1; BSD-TDR-63-124)
(Contract AF 04(695)-169) Unclassified Report

A number of instruments for probing the plasma sheath during reentry are described. The instruments respond to the induced magnetic field produced by the interaction of the ionized gas flowing through an applied magnetic field. Flight models to measure the product of electrical conductivity and velocity, σu, and the σu profile are discussed. In addition analysis and description of laboratory transducers for determining velocity, σu fluctuations, and average electron collision frequency are presented.

UNCLASSIFIED

UNCLASSIFIED

Aerospace Corporation, El Segundo, California. FLIGHT INSTRUMENTATION FOR REENTRY PLASMA SHEATH, prepared by Allen E. Fuhs. 12 July 1963. [46]p. incl. illus.
(Report TDR-169(3153-20)TN-1; BSD-TDR-63-124)
(Contract AF 04(695)-169) Unclassified Report

A number of instruments for probing the plasma sheath during reentry are described. The instruments respond to the induced magnetic field produced by the interaction of the ionized gas flowing through an applied magnetic field. Flight models to measure the product of electrical conductivity and velocity, σu, and the σu profile are discussed. In addition analysis and description of laboratory transducers for determining velocity, σu fluctuations, and average electron collision frequency are presented.

UNCLASSIFIED

UNCLASSIFIED

UNCLASSIFIED

UNCLASSIFIED

UNCLASSIFIED

UNCLASSIFIED

UNCLASSIFIED

UNCLASSIFIED

UNCLASSIFIED